

# Valence bond crystal in a pyrochlore antiferromagnet with orbital degeneracy

S. Di Matteo,<sup>1,2</sup> G. Jackeli,<sup>3,\*</sup> C. Lacroix,<sup>4</sup> and N. B. Perkins<sup>1,5</sup>

<sup>1</sup>Laboratori Nazionali di Frascati INFN, via E. Fermi 40, C.P. 13, I-00044 Frascati (Roma) Italy

<sup>2</sup>Dipartimento di Fisica, Università di Roma III, via della Vasca Navale 84, I-00146 Roma Italy

<sup>3</sup>Institut Laue Langevin, B. P. 156, F-38042, Grenoble, France

<sup>4</sup>Laboratoire L. Néel, CNRS, BP 166, 38042 Grenoble Cedex 09, France

<sup>5</sup>Bogoliubov Laboratory of Theoretical Physics, JINR, 141980, Dubna, Russia

(Dated: October 29, 2018)

We discuss the ground state of a pyrochlore lattice of threefold-orbitally-degenerate  $S = 1/2$  magnetic ions. We derive an effective spin-orbital Hamiltonian and show that the orbital degrees of freedom can modulate the spin exchange, removing the infinite spin-degeneracy characteristic of pyrochlore structures. The resulting state is a collection of spin-singlet dimers, with a residual degeneracy due to their relative orientation. This latter is lifted by a magneto-elastic interaction, induced in the spin-singlet phase-space, that forces a tetragonal distortion. Such a theory provides an explanation for the helical spin-singlet pattern observed in the B-spinel  $\text{MgTi}_2\text{O}_4$ .

PACS numbers: 75.10.Jm, 75.30.Et

Geometrically frustrated antiferromagnets have reached an increasing interest in the past decade [1]. The reason is that their ground states are highly degenerate and can evolve in a variety of ways: they can remain liquid down to the lowest temperatures due to quantum effects [2], or lift their degeneracy via the order-out-of-disorder mechanism [3], or through a phase transition that lowers the local symmetry of the lattice [4, 5]. In this Letter we want to point out and discuss another scenario, that can appear when magnetic ions of frustrated lattices possess also an orbital degeneracy. The physical behavior of such systems may be drastically different from that of pure spin models, as the occurrence of an orbital ordering can modulate the spin exchange, thus lifting the geometrical degeneracy of the underlying lattice. In the following we focus on a system with threefold-orbitally-degenerate  $S = 1/2$  magnetic ions in a corner-sharing tetrahedral (pyrochlore) lattice. This model is suitable to describe  $d^1$ -type transition-metal compounds, like the B-spinel  $\text{MgTi}_2\text{O}_4$ . Here the magnetically active  $\text{Ti}^{3+}$ -ions form a pyrochlore lattice and are characterized by one single electron in the threefold degenerate  $t_{2g}$ -manifold.  $\text{MgTi}_2\text{O}_4$  undergoes a metal-to-insulator transition on cooling below 260 K, with an associated cubic-to-tetragonal lowering of the symmetry [6]. At the transition the magnetic susceptibility continuously decreases and saturates, in the insulating phase, to a value which is anomalously small for spin  $1/2$  local moments: for this reason the insulating phase has been interpreted as a spin-singlet. Subsequent synchrotron and neutron powder diffraction experiments have revealed that the low-temperature crystal structure is made of alternating short and long Ti-Ti bonds forming a helix about the tetragonal  $c$ -axis [7]. These findings have suggested a removal of the pyrochlore degeneracy by a one-dimensional (1D) helical dimerization of the spin pattern, with spin-singlets

located on short bonds. This phase can be regarded as a valence bond crystal (VBC) since the long-range order of spin-singlets (dimers) extends throughout the whole pyrochlore lattice.

Here we describe the microscopic theory behind the stabilization of this VBC ground state. We argue that, remarkably, such a novel phase can be realized on a pyrochlore lattice because of orbital degeneracy, without invoking any exotic interactions. The existence of orbitally-driven VBC had been suggested for cubic lattice of  $d^9$  compounds [8]. For  $d^2$  compounds with frustrated lattices, the orbital order is shown to induce a spin-singlet ground state, for triangular lattices [9], or a spin ordered one, for pyrochlore lattices [10]. Yet, the peculiar case of  $d^1$  spinel compounds leads to new results: the onset of an orbitally driven VBC state on the pyrochlore lattice.

*Effective Hamiltonian:* We first derive a superexchange spin-orbital Hamiltonian à la Kugel-Khomskii (KK) [11] for threefold orbitally-degenerate  $d^1$ -ions on a pyrochlore lattice. We assume that the low-temperature insulating phase of  $\text{MgTi}_2\text{O}_4$  is of Mott-Hubbard type. We work in the cubic crystal class and look for possible instabilities towards symmetry reductions. Our parameters are the nearest-neighbor (NN) hopping term  $t$ , the Coulomb on-site repulsions  $U_1$  (within the same orbital) and  $U_2$  (among different orbitals), and the Hund's exchange,  $J_H$ . For  $t_{2g}$  wavefunctions the relation  $U_1 = U_2 + 2J_H$  holds due to rotational symmetry in real space. The orbital occupancies of  $t_{2g}$  orbitals,  $n_{\alpha\beta}$  ( $\alpha, \beta = x, y, z$ ), are expressed in terms of the pseudospin  $\vec{\tau} = 1$ , with the correspondence:  $\tau^z = -1 \rightarrow |yz\rangle$ ,  $\tau^z = 0 \rightarrow |xy\rangle$ , and  $\tau^z = 1 \rightarrow |xz\rangle$ . At first, we consider only the leading part of the hopping term, due to the largest  $dd\sigma$  element, and discuss later the effects of smaller contributions (e.g.  $dd\pi$ ). The  $dd\sigma$  overlap in  $\alpha\beta$  plane connects only the corresponding orbitals of the same  $\alpha\beta$  type. Thus, the total number of electrons in each orbital state is a conserved

quantity and the orbital part of the effective Hamiltonian  $H_{\text{eff}}$  is Ising-like:

$$H_{\text{eff}} = -J_1 \sum_{\langle ij \rangle} [\vec{S}_i \cdot \vec{S}_j + 3/4] O_{ij} \quad (1)$$

$$+ J_2 \sum_{\langle ij \rangle} [\vec{S}_i \cdot \vec{S}_j - 1/4] O_{ij} + J_3 \sum_{\langle ij \rangle} [\vec{S}_i \cdot \vec{S}_j - 1/4] \tilde{O}_{ij}$$

where the sum is restricted to the NN sites. Introducing the projectors on the orbital states of site  $i$ ,  $P_{i,xz} = \frac{1}{2}\tau_{iz}(1 + \tau_{iz})$ ,  $P_{i,xy} = (1 - \tau_{iz})(1 + \tau_{iz})$  and  $P_{i,yz} = -\frac{1}{2}\tau_{iz}(1 - \tau_{iz})$ , the orbital contributions along the bond  $ij$  in  $\alpha\beta$ -plane is given by  $O_{ij} = P_{i,\alpha\beta}(1 - P_{j,\alpha\beta}) + P_{j,\alpha\beta}(1 - P_{i,\alpha\beta})$  and  $\tilde{O}_{ij} = P_{i,\alpha\beta}P_{j,\alpha\beta}$ . The first and second terms in  $H_{\text{eff}}$  describe the ferromagnetic (FM)  $J_1 = t^2/(U_2 - J_H)$  and the antiferromagnetic (AFM)  $J_2 = t^2/(U_2 + J_H)$  interactions, respectively, and are active only when the two sites involved are occupied by different orbitals. The last term is AFM, with  $J_3 = \frac{4}{3}t^2[2/(U_2 + J_H) + 1/(U_2 + 4J_H)]$ , and is non-zero only when the two sites have the same orbital occupancy. At this point it is useful to have an idea of the energy scales that play a role in the Hamiltonian (1). We estimate  $t \equiv t_\sigma \simeq 0.32$  eV,  $J_H \simeq 0.64$  eV and  $U_2 \simeq 4.1$  eV [12]. Thus  $\eta = J_H/U_2 \simeq 0.15 \ll 1$  and, just in order to present the results in a more transparent form, we expand the exchange energies around  $\eta = 0$ . We get  $J_1 \simeq J(1 + \eta)$ ,  $J_2 \simeq J(1 - \eta)$  and  $J_3 \simeq 4J(1 - 2\eta)$  where  $J = t^2/U_2 \simeq 25$  meV represents the overall energy scale. In the following we measure all energies in units of  $J$ .

The main aspect of  $H_{\text{eff}}$  is that, due to  $dd\sigma$ -character of the hopping terms, only some orbital configurations contribute to the energy: every bond  $ij$  in the  $\alpha\beta$  plane has zero energy gain unless at least one of the two sites  $i$  and  $j$  has an occupied  $\alpha\beta$  orbital. The strength, as well as the sign, of spin-exchange energy associated with two NN sites  $i$  and  $j$  depends on their orbital occupations and the direction of the  $ij$  bond. The strongest bond in the generic  $\alpha\beta$ -plane is characterized by both sites with  $\alpha\beta$  occupancy: we shall call it  $b_0$ . Its exchange interaction is AFM and its spin Hamiltonian is given by:

$$H_{b_0} = -1 + 2\eta + 4[1 - 2\eta]\vec{S}_i \cdot \vec{S}_j. \quad (2)$$

When the two sites of bond  $ij$  in  $\alpha\beta$ -plane are occupied by one  $\alpha\gamma$  and one  $\alpha\beta$  orbitals,  $\gamma \neq \beta$  (bond  $b_1$ ), one gets a weak FM interaction:

$$H_{b_1} = -1 - \eta/2 - 2\eta\vec{S}_i \cdot \vec{S}_j. \quad (3)$$

Finally, the two sites of bond  $ij$  in  $\alpha\beta$ -plane can be occupied by one  $\alpha\gamma$  and one  $\beta\gamma$  orbitals (bond  $b_2$ ), or, by two  $\alpha\gamma$  (or  $\beta\gamma$ ) orbitals (bond  $b_3$ ). These bonds are non-interacting, as far as only  $dd\sigma$  overlap is considered.

*Single tetrahedron:* In one tetrahedron there are basically three possible orbital configurations to be considered (see Fig. 1): A) all four sites have the same orbital

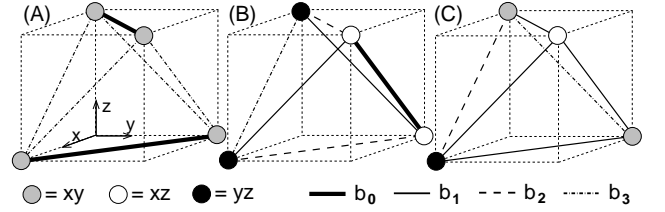


FIG. 1: Orbital and bond arrangements on a tetrahedron for cases A), B) and C).

occupancy (say  $xy$ ) and thus only the two bonds in  $xy$ -plane (shown by solid lines in Fig. 1A) give a non-zero energy contribution; B) the two sites in one  $\alpha\beta$ -plane, e.g.  $xz$ , are both occupied by  $xz$  orbitals, while at least one of the two sites in the other  $xz$ -plane is occupied by  $xy$  or  $yz$  orbitals (Fig. 1B); C) no bonds  $ij$  in the plane  $\alpha\beta$  of the tetrahedron is such as to have both sites occupied by the  $\alpha\beta$ -orbital (Fig. 1C). These three configurations are the bricks that allow to build the orbital pattern throughout the whole pyrochlore lattice. Because of the Ising-form of orbital interactions, in the following we can focus simply on these three cases, relying on the fact that configurations with a linear superposition of orbitals on each site must have a higher energy. We shall do only one exception to study a case with a particular physical meaning, i.e., that of a "cubic" symmetry, where each site is occupied by a linear superposition with equal weights of the three orbitals  $\frac{1}{\sqrt{3}}[|xy\rangle + |xz\rangle + |yz\rangle]$ , (case D).

*Pyrochlore lattice:* Here we consider possible coverings of the pyrochlore lattice through the various tetrahedra.

A) **Heisenberg chains** - When all tetrahedra of pyrochlore lattice are of type A (ferro-orbital ordering) then the effective Hamiltonian (1) can be mapped into a set of one dimensional decoupled Heisenberg chains. If, for example, all occupied orbitals are of  $xy$ -type, all chains in  $(1, \pm 1, 0)$  cubic directions (see Fig. 1A) are decoupled. The only interactions are due to AFM  $b_0$ -bonds described by the spin Hamiltonian (2). Thus, the ground-state energy per site can be evaluated exactly by using the results for an Heisenberg 1D-chain [13]:  $E_A = -2.77(1 - 2\eta)$ .

B) **Dimer phase** - This state is made of B-type tetrahedra. We distinguish three types of such tetrahedra. All three are characterized by one strong  $b_0$  bond, in a  $\alpha\beta$  plane. The other two ions in the opposite  $\alpha\beta$ -plane can either be occupied by two  $\alpha\gamma$  ( $\beta\gamma$ ) orbitals, forming a  $b_3$  bond, (case  $B_1$ , the one shown in Fig. 1B), or by one  $\alpha\gamma$  and one  $\alpha\beta$  orbitals, linked in a  $b_1$  bond, (case  $B_2$ ), or, finally, by one  $\alpha\gamma$  and one  $\beta\gamma$  orbitals, forming a  $b_2$  bond, (case  $B_3$ ). Since  $b_2$  and  $b_3$  bonds do not contribute to the energy, this latter depends only on the number,  $n_{b_0}$  and  $n_{b_1}$ , of  $b_0$  and  $b_1$  bonds in the unit cell. As all three  $B_i$  configurations are characterized by  $n_{b_0} = 1$  and  $n_{b_1} = 2$ , all possible coverings of pyrochlore lattice by  $B_i$  tetrahedra have the same energy, even if  $(n_{b_2}, n_{b_3})$  are different for three  $B_i$  tetrahedra ((2,1) for  $B_1$ ; (1,2) for

$B_2$ ; (3,0) for  $B_3$ ). When pyrochlore lattice is covered by  $B_i$ -types tetrahedra (two possible coverings are shown in Fig. 2), then each spin is engaged in one strong AFM  $b_0$  bond Eq. (2), and two weak FM  $b_1$ -bonds Eq. (3). Such coverings form a degenerate manifold and the corresponding energy can be calculated as follows. In the limit  $\eta \rightarrow 0$ , the spin-only Hamiltonian can be solved exactly, as it can be decomposed into a sum of spin-uncoupled  $b_0$  bonds. In this case the energy minimum is reached when the Heisenberg term of the  $b_0$ -bond is the lowest, i.e., for a pure quantum spin-singlet ( $\vec{S}_i \cdot \vec{S}_j = -3/4$ ). Remarkably, such spin-singlet (dimer) states, in the limit  $\eta \rightarrow 0$ , are also exact eigenstates of the full Hamiltonian (1). As  $\eta \ll 1$ , the dimer state is stable against the weak FM interdimer interaction. In this case the magnetic contribution along the FM  $b_1$ -bond is zero ( $\langle \vec{S}_i \cdot \vec{S}_j \rangle = 0$  for  $i$  and  $j$  belonging to different dimers) and we are led to an energy per site given by:  $E_B = E_{b_0}/2 + E_{b_1} = -3 + \frac{7}{2}\eta$ . Here  $E_{b_{0(1)}}$  is the energy of the bond  $b_{0(1)}$ .

**C) FM order:** Consider the state where all tetrahedra are of type  $C$  (see Fig. 1C). There are four interacting  $b_1$  bonds and two noninteracting bonds ( $b_2$  and  $b_3$ ) per tetrahedron. All non zero spin-exchanges are FM given by Eq. (3). The ground state for this case is, thus, ferromagnetic with an energy  $E_C = 2E_{b_1} = -2(1 + \eta)$ .

**D) Frustrated AFM:** The realization of this phase restores the full pyrochlore lattice symmetry, thus describing an ideal cubic phase. All bonds are equivalent and by averaging Eq. (1) over the orbital configurations on neighboring sites  $i$  and  $j$ , we obtain the spin Heisenberg Hamiltonian on the pyrochlore lattice:  $H_D = \sum_{\langle ij \rangle} (-5/9 + [4/9 - 16\eta/9]\vec{S}_i \cdot \vec{S}_j)$ . The system is thus highly frustrated and its ground state is a spin-liquid [2], whose energy per site is:  $E_D \simeq -1.89 + 0.89\eta$ . Here we have used the ground-state energy estimated  $(1/N) \sum_{ij} \vec{S}_i \cdot \vec{S}_j \simeq -0.5$  on the pyrochlore lattice [14].

**E) Mixed A and C configuration:** It is possible to cover the pyrochlore lattice also by means of a mixed configuration with  $A$  and  $C$  types tetrahedra. It can be visualized from Fig. 2b if, e.g., the four labeled tetrahedra would be of A-type, with two spin-singlets on strong  $b_0$  bonds and three different orbital occupancy, and the four unlabeled tetrahedra of C-type with no spin-singlets. This dimer configuration is degenerate with the B-phase as far as only  $dd\sigma$  overlap is considered, as, in average,  $n_{b_0} = 1$  and  $n_{b_1} = 2$ . Yet, in this case  $n_{b_2} = 1/2$  and  $n_{b_3} = 5/2$  and the degeneracy is removed by  $dd\pi$  overlap in favor of the B-phase (for which  $n_{b_2} \geq 1$ ), as the energy gain of the  $b_2$  bond is  $-t_\pi^2/[4t^2]$  (in units of  $J$ ), while that of the  $b_3$  bond is  $-t_\pi^2/[8t^2]$ .

**Ground state manifold:** On the basis of the previous energy considerations, a simple phase diagram can be derived, in terms of  $\eta$ , the only free parameter available. For  $\eta = 0$  the lowest ground-state energy is that of phase  $B$ . With increasing  $\eta$  we find only one phase transition at  $\eta_c = 2/11 \simeq 0.18$ , between dimer-phase  $B$  and FM phase

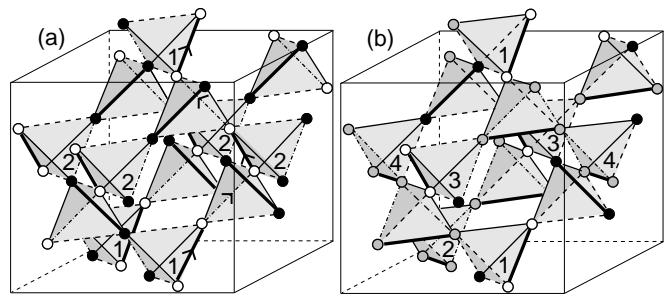


FIG. 2: Two different coverings of the unit cubic cell through dimers, phase  $B$ . The same notations as in Fig. 1 are used. Locations of singlets are represented by thick links. Different numbers correspond to inequivalent tetrahedra. (a) The experimental phase of  $\text{MgTi}_2\text{O}_4$ : the helical dimerization pattern (indicated by arrows) is formed by alternating short  $b_0$  and long  $b_3$  bonds. All tetrahedra are in phase  $B_1$ ; (b) a different covering of the cubic cell through all  $B_i$  tetrahedra. The inclusion of the magneto-elastic coupling pushes these states higher in energy.

**C.** As  $\eta_c$  is above our estimated value of  $\eta \simeq 0.15$ , we can conclude that the ground state of  $\text{MgTi}_2\text{O}_4$  is described by the phase  $B$  and is characterized by a frozen pattern of spin-singlets throughout the whole pyrochlore lattice that removes the original spin degeneracy. Nonetheless, there is still a remaining degeneracy to be lifted. It is related to the freedom in the choice of the two orbitals on the tetrahedron bond opposite to the one of the singlet. Different choices of these orbitals give rise to inequivalent covering patterns of the pyrochlore lattice with one dimer per tetrahedron (see Fig. 2). This degeneracy is given by the number of such dimer coverings and the corresponding number of states can be estimated to grow with the system size as  $\mathcal{N} \sim 3^{N_T} = \sqrt{3}^N$  [15]. Here  $N_T = N/2$  is the number of tetrahedra and we have ignored the contributions coming from closed loops (hexagons) on the pyrochlore lattice. This ground state manifold is different from a resonating valence bond state, since each dimer covering is frozen in an exact eigenstate of the Hamiltonian (1) for  $\eta = 0$ . For finite  $\eta$  the different dimer patterns are not connected by Hamiltonian: the bond corresponding to the dimer in each tetrahedron is fixed, being determined by orbital pattern and orbital degrees of freedom are Ising-like variables. Thus a tunneling between different dimer states cannot occur.

**Lifting of degeneracy:** The above discussed degeneracy can not be removed within the KK-type model, not even introducing  $dd\pi$  and  $dd\delta$  overlaps. The reason is related to the fact that the energy gain depends only on the total number of each type of bond ( $n_{b_0}, n_{b_1}, n_{b_2}, n_{b_3}$ ) in the unit cell and, in order to fill the whole crystal with a periodicity not lower than the one of the primitive cubic cell shown in Fig. 2, the average number of bonds  $n_{b_i}$  per tetrahedron is the same, whichever of the three building blocks  $B_1, B_2$ , or  $B_3$  is used. It is given by  $n_{b_0} = 1$ ,

$n_{b_1} = 2, n_{b_2} = 2, n_{b_3} = 1$ , and it corresponds to the value of case  $B_1$ , that is the only one that allows to cover the whole cubic cell without mixing to other configurations (see Fig. 2a). Associated to the  $B_1$ -phase, we have the minimal cell enlarging (doubling instead of quadrupling), and the maximal space subgroup ( $P4_12_12$ ) of the original face-centered  $Fd\bar{3}m$  cubic cell.

In order to substantiate these geometrical considerations, we need to find the physical mechanism that removes the  $B$ -manifold degeneracy in favor of the  $B_1$ -state. From the above discussion it follows that only correlations between bonds can lift it. These correlations naturally appear if the magneto-elastic contribution to the energy is considered, as the orbitally-driven modulations of the spin exchange energies distort the underlying lattice through the spin-Peierls mechanism. In the degenerate  $B$ -manifold, every tetrahedron is characterized by a strong exchange on the bond  $b_0$  where the singlet is located. A reduction of the bond length enlarges the energy gain, because of the increase in the  $dd\sigma$  overlap. This selects the triplet-T deformation mode from the irreducible representations of the tetrahedron group, which is the only one that singles out one shorter bond [16]. This mode generates a tetragonal distortion of the tetrahedron, with short and long bonds located opposite to each other and four intermediate bonds. Due to this mechanism, the position of the two  $b_1$ -bonds in the tetrahedron is uniquely determined: in order to maximize the superexchange energy gain by keeping the highest value for  $t_\sigma$ , the intermediate-strength  $b_1$ -bonds are not allowed to lie on the long bond opposite to the singlet  $b_0$ . The elongation of the weak bonds of  $b_3$  type is energetically more favorable. It is possible to check that the only possibility to have such a constraint for the whole cell is realized for the state  $B_1$  (Fig. 2a). On the contrary, both cases  $B_2$  and  $B_3$  (Fig. 2b), do not allow to cover the cell without at least one  $b_1$ -bond lying opposite to the singlet edge (e.g. tetrahedron 4 in Fig. 2b), thus with an extra-energy cost. Hence, the energy is minimized when all tetrahedra are of  $B_1$  kind, with a  $T$ -type tetragonal distortion. In this state all dimers are condensed in the ordered helical pattern shown in Fig. 2a and form a VBC. This dimerization pattern exactly reproduces the one observed in the insulating phase of  $MgTi_2O_4$  [7]. The present theory also predicts a peculiar orbital ordering in the dimerized phase: a ferro-type order along the helices with antiferro-type order between them (see Fig. 2a). This orbital ordering can undergo an experimental test through Ti K edge natural circular dichroism, which is sensitive to the chirality of  $t_{2g}$  orbital order along the helix, when x-rays are shone along the helical axis.

Within the present scenario two transition temperatures are expected. The highest  $T_{c_1}$ , determined by the exchange coupling within the singlet ( $T_{c_1} \sim J_3 \simeq 4J \simeq 1000K$ ), corresponds to the transition from a paramagnet to a spin gap (dimer) state, with a ferro-orbital order

on each dimer. This state can be regarded as a weakly-interacting gas of dimers and is highly degenerate with respect to the dimers orientation. The lowest transition temperature, given by the magneto-elastic coupling, lifts the degeneracy through the spin-Peierls distortion. At this temperature dimers condense and form the VBC shown in Fig.2a. The entropy involved in this transition is estimated to be  $\sim \ln[N]/N = \ln\sqrt{3}$ . In the case of  $MgTi_2O_4$ , it is known [6] that, with increasing temperature, this compound goes from an insulating to a metallic phase at  $T_{c_2} \simeq 260K$ . The transition to the metallic state rules out the possibility of a high-temperature spin-singlet state with disordered dimers and does not allow to evaluate the order of magnitude of the magneto-elastic coupling. We can just estimate its lower limit as about  $1/4(\simeq T_{c_2}/T_{c_1})$  of the singlet-binding energy.

In summary, we have derived a mechanism that allows to lift the geometrical degeneracy of a pyrochlore lattice of threefold-orbitally-degenerate  $t_{2g}$ , spin-1/2 magnetic ions like  $Ti^{3+}$ . We have singled out two relevant energy scales that govern its behavior: the main one is the superexchange energy gain, that drives the system into a spin-singlet dimer state with peculiar orbital pattern. The residual orientational degeneracy is then lifted through the magneto-elastic interaction that optimizes the previous energy gain by distorting the bonds in the suitable directions and leading to a tetragonal distortion. This generates a condensate of dimers in a VBC state, forming 1D dimerized helical chains running around the tetragonal  $c$ -axis, the one actually observed in  $MgTi_2O_4$ .

---

\* Also at E. Andronikashvili Institute of Physics, Georgian Academy of Sciences, Tbilisi, Georgia.

- [1] A.P. Ramirez in *Handbook of Magnetic Materials*, edited by K. H. J. Buschow (North-Holland, Amsterdam, 2001).
- [2] B. Canals and C. Lacroix, *Phys. Rev. Lett.* **80**, 2933 (1998); H.Tsunetsugu, *Phys. Rev. B* **65**, 024415, (2001).
- [3] J. Villain *et al.*, *J. Phys. (Paris)* **41**, 1263 (1980).
- [4] Y. Yamashita and K. Ueda, *Phys. Rev. Lett.* **85**, 4960 (2000).
- [5] O. Tchernyshyov, R. Moessner, and S. L. Sondhi, *Phys. Rev. B* **66**, 064403 (2002).
- [6] M. Isobe and Y. Ueda, *J. Phys. Soc. Jpn.* **71**, 1848 (2002).
- [7] M. Schmidt *et al.*, *Phys. Rev. Lett.* **92**, 056402 (2004).
- [8] L.F. Feiner, A.M. Oles, and J. Zaanen, *Phys. Rev. Lett.* **78**, 2799 (1997).
- [9] H. F. Pen *et al.*, *Phys. Rev. Lett.* **78**, 1323 (1997).
- [10] H. Tsunetsugu, Y. Motome, *Phys. Rev. B* **68**, 060405(R) (2003); O. Tchernyshyov, *cond-mat/0401203*
- [11] K. I. Kugel and D. I. Khomskii, *Usp. Fiz. Nauk* **136**, 621 (1982), [*Sov. Phys. Usp.* 25, **231** (1982)].
- [12] T. Mizokawa and A. Fujimori, *Phys. Rev. B* **54**, 5368 (1996); J. Matsuno, A. Fujimori, and L.F. Mattheiss, *ibid.* **60**, 1607 (1999)
- [13] M. Takhshi, *Thermodynamics of One-Dimensional Solvable Models*, (Cambridge University Press, 1999).

- [14] B. Canals and C. Lacroix, Phys. Rev. B **61**, 1149 (2000).
- [15] When a singlet is located on a given tetrahedron then each neighboring tetrahedron is left with only three possible choices for a singlet location.
- [16] For a simple spin Hamiltonian it is the doublet  $E$ -mode that removes the local degeneracy of the tetrahedron [4].